Proc. Natl. Acad. Sci. USA
Vol. 93, pp. 6361–6366, June 1996
Neurobiology

Targeted deletion in astrocyte intermediate filament (*Gfap*) alters neuronal physiology

(long-term potentiation/hippocampus/optic nerve/homologous recombination/mouse)

M. A. McCALL*, R. G. GREGG†, R. R. BEHRINGER‡, M. BRENNER§, C. L. DELANEY*¶, E. J. GALBREATH*, C. L. ZHANG‖, R. A. PEARCE**, S. Y. CHIU‖, AND A. MESSING*††

Departments of *Pathobiological Sciences, **Anesthesiology/Anatomy, and ‖Neurophysiology, ¶Neuroscience Training Program, and †Waisman Center, University of Wisconsin–Madison, Madison, WI 53706; ‡M.D. Anderson Cancer Center, Houston, TX 77030; and §Stroke Branch, National Institute of Neurological Disorders and Stroke, National Institutes of Health, Bethesda, MD 20892

Communicated by R. L. Brinster, University of Pennsylvania, Philadelphia, PA, February 28, 1996 (received for review January 24, 1996)

ABSTRACT **Glial fibrillary acidic protein (GFAP) is a member of the family of intermediate filament structural proteins and is found predominantly in astrocytes of the central nervous system (CNS). To assess the function of GFAP, we created GFAP-null mice using gene targeting in embryonic stem cells. The GFAP-null mice have normal development and fertility, and show no gross alterations in behavior or CNS morphology. Astrocytes are present in the CNS of the mutant mice, but contain a severely reduced number of intermediate filaments. Since astrocyte processes contact synapses and may modulate synaptic function, we examined whether the GFAP-null mice were altered in long-term potentiation in the CA1 region of the hippocampus. The GFAP-null mice displayed enhanced long-term potentiation of both population spike amplitude and excitatory post-synaptic potential slope compared to control mice. These data suggest that GFAP is important for astrocyte-neuronal interactions, and that astrocyte processes play a vital role in modulating synaptic efficacy in the CNS. These mice therefore represent a direct demonstration that a primary defect in astrocytes influences neuronal physiology.**

Astrocytes and their precursors serve a number of functions in the mammalian central nervous system (CNS) (for review see ref. 1). During development, radial glia appear early and guide subsequent migration of neurons as well as outgrowth of neuronal dendrites and axons. More mature astrocytes may influence the development of oligodendrocytes and endothelium. In the adult nervous system, astrocytes provide structural support to surrounding cells, regulate the ionic and neurotransmitter levels in the extracellular fluid, and secrete pleiotropic growth factors. In this manner astrocytes likely influence the physiological properties of adjacent neurons.

One of the key events during astrocyte differentiation is the onset of expression of the intermediate filament glial fibrillary acidic protein (GFAP). Astrocyte precursors initially express vimentin, switching to GFAP as they mature (2, 3). Neurons make a similar switch from vimentin to the three neurofilaments during their differentiation (4). GFAP is considered a unique marker for astrocytes in the CNS, but it is also present in several other cell types in the periphery, particularly nonmyelinating Schwann cells of the peripheral nervous system (5–7). The levels of GFAP markedly increase during reactive gliosis when astrocytes undergo both hypertrophy and hyperplasia (for review see ref. 8). Recent studies of either forced overexpression or antisense inhibition of GFAP expression in cultured cells suggest a direct role for GFAP in controlling outgrowth of processes by astrocytes (9–11).

The publication costs of this article were defrayed in part by page charge payment. This article must therefore be hereby marked "*advertisement*" in accordance with 18 U.S.C. §1734 solely to indicate this fact.

Recently, two groups reported that targeted mutations in the *Gfap* gene do not interfere with mouse development (12, 13). Preliminary studies of astrocyte numbers and morphology in these mice indicated little change, but morphology in particular has been difficult to assess in the absence of GFAP, which itself has been the standard marker for visualizing astrocytes at the light microscopic level. Upon injury, GFAP-deficient astrocytes appeared to initiate at least some of the molecular changes typical of reactive astrocytes. Given the many proposed interactions between astrocytes and neurons, changes in astrocyte structure or function might lead to changes in neuronal physiology. We have also generated GFAP-null mice using homologous recombination in embryonic stem (ES) cells. We report here that GFAP-null mice have subtle changes in astrocyte morphology, and in addition show enhanced long-term potentiation (LTP) in hippocampal neurons.

MATERIALS AND METHODS

Construction of the Targeting Vector. The GFAP targeting vector was constructed from a genomic clone isolated from a 129/SvEv genomic library (Stratagene no. 946305), and is shown diagrammed in Fig. 1, along with the endogenous mouse locus and the final mutant allele. The targeting vector contains PGK*neo*bpA (14) inserted into the *Sal*I site in the first exon of the *Gfap* gene, and a MC1 thymidine kinase gene attached at the 3′ end for negative selection against nonhomologous recombinants. In addition to interrupting the open reading frame in exon 1 by insertion of the *neo* gene, the internal *Sal*I–*Xba*I fragment was deleted to eliminate most of exon 1 and all of exons 2–4. The targeting vector contained a 2.2-kb 5′ arm of homology (*Bam*HI–*Sal*I fragment) and a 1.4-kb 3′ arm of homology (*Xba*I–*Bam*HI fragment). Probes used for Southern blot analysis of targeted clones included: GFAP 3′ probe = 600-bp *Bam*HI–*Eco*RI fragment; *neo* probe = 0.9-kb *Pst*I–*Not*I fragment.

Creation of Targeted ES Cells and GFAP-Null Mice. AB-1 ES cells were electroporated with 10 μg of linearized targeting vector and treated with G418 (350 μg/ml) and 1-(2-deoxy-2-fluoro-β-D-arabinofuranosyl)-5-iodouracil (FIAU) (200 nM) for selection of doubly resistant colonies. Southern blot analyses were performed as described (15) on DNA digested with *Eco*RI (for 3′ probe) or *Eco*RV (for *neo* probe). Targeted ES cell clones were injected into C57BL/6J (B6) blastocysts (University of Cincinnati Embryonic Stem Cell Core Facility)

Abbreviations: PS, population spike; EPSP, excitatory postsynaptic potential; GFAP, glial fibrillary acidic protein; CNS, central nervous system; LTP, long-term potentiation; ES, embryonic stem; H&E, hematoxylin/eosin.

††To whom reprint requests should be addressed at: School of Veterinary Medicine, University of Wisconsin–Madison, 2015 Linden Drive, Madison, WI 53706. e-mail: amessing@svm.vetmed.wisc.edu.

to generate chimeric founder mice. Founder mice were bred either to inbred B6 mice to maintain the mutation on a hybrid background, or to 129/SvJ mice to maintain the mutation on a 129 genetic background. The mice described in this report have been given the strain designation *Gfap*^{tm1Mes}.

Northern Blot Analysis of GFAP, Vimentin, and Nestin Expression. RNA was prepared by homogenization of whole brain in guanidinium isothiocyanate and centrifugation through CsCl (16). For Northern blot analysis, 10 μg of total RNA from each tissue was fractionated on a 1.2% agarose-formaldehyde gel and blotted to nitrocellulose (16). Equal loading of samples was confirmed by ethidium bromide staining. Membranes were hybridized with probes derived from either a mouse GFAP cDNA (pG1, gift of N. J. Cowan) (17), human vimentin cDNA (4F1, gift of V. Lee) (18), or rat nestin cDNA (401:6, gift of R. McKay) (19). Probes were labeled with ^{32}P by random priming, and hybridization carried out at 42°C in Fast Pair (Digene Diagnostics, Beltsville, MD). Filters were washed as described (16), except that an additional wash with 0.1× SSPE/0.1% SDS at 55°C was used for the vimentin Northern blot. Blots were exposed at −70°C for 4 days (GFAP) or 7 days (vimentin and nestin).

Light and Electron Microscopy. For light microscopic analysis, mice were anesthetized with Avertin and perfused transcardially with 0.1 M PBS (pH 7.4) followed by 4% paraformaldehyde in PBS [for hematoxylin/eosin (H&E) or GFAP] or acid-alcohol (for vimentin). The brains were removed, postfixed overnight, and embedded in paraffin. Sections (5 μm) were cut, and prepared either for staining with H&E or for immunohistochemical detection of either GFAP or vimentin. For electron microscopic analysis, mice were perfused with PBS followed by 2% paraformaldehyde/2.5% glutaraldehyde in 0.1 M cacodylate, pH 7.4 (n = 3 wild type, 3 nulls). The brains, optic and sciatic nerves were removed and postfixed in the same glutaraldehyde solution overnight. All tissues were postfixed with 1% osmium tetroxide for 30 min, dehydrated, and embedded in Epon. Thin sections (70–90 nm) were stained with lead citrate and uranyl acetate, and photographed with a Philips 410 electron microscope.

Immunohistochemical Analysis of GFAP and Vimentin. Deparaffinized sections were rehydrated through a graded series of ethanol, quenched in 95% methanol/0.01% hydrogen peroxide, and blocked with 3% normal goat serum in PBS. The sections were incubated with primary antibodies diluted in 1% normal goat serum/PBS either for 1 hr at room temperature or overnight at 4°C. Dilutions of primary antibodies were 1:250 for anti-GFAP (Dako) and 1:200 for anti-vimentin (20). After incubation in the primary antibody, the sections were washed with PBS and processed with the Vector Elite system (Vector Laboratories).

Electrophysiological Analysis of Synaptic Function. Excitatory synaptic transmission and potentiation (LTP) were examined in area CA1 of hippocampal slices prepared from mutant and control mice. Mice were anesthetized with ether, decapitated, and the brain rapidly removed into ice-cold artificial cerebrospinal fluid containing: 127 mM NaCl/1.9 mM KCl/1.2 mM KH_2PO_4/2.2 mM $CaCl_2$/1.4 mM $MgSO_4$/26 mM $NaHCO_3$/and 10 mM glucose, bubbled with 95% O_2/5% CO_2, pH 7.40. The hippocampus was dissected free of the surrounding brain, and 400-μm vibratome sections were cut from the middle third in artificial cerebrospinal fluid at approximately 4°C. Slices were maintained at room temperature in a submerged holding chamber for at least 1 hr prior to transfer to a submersion style recording chamber, continuously perfused with artificial cerebrospinal fluid (also at room temperature) at 3 cc/min. The population spike (PS) and excitatory postsynaptic potential (EPSP) were recorded simultaneously with two glass microelectrodes filled with NaCl (2 M, tip broken to 2–5 MΩ) placed into stratum pyramidale and stratum radiatum, respectively. Constant current electrical stimuli of 0.1 ms duration were delivered to the Schaffer collateral pathway using a monopolar tungsten stimulating electrode placed in the stratum radiatum. Stimulus strength was adjusted to produce a PS approximately one-third of maximum amplitude, generally requiring 50–150 μamps. This fixed intensity was used both to monitor evoked responses and to induce LTP by a series of three 100-Hz trains, each lasting 1 sec, repeated at 10-sec intervals. Test responses were evoked every 60 sec, amplified using an Axoclamp 2A amplifier (Axon Instruments, Foster City, CA), and acquired and analyzed using pClamp v.6. Responses were recorded for 10–40 min, until stable baseline responses were observed, and for at least 60 min following LTP induction. Data were analyzed by an individual (C.L.Z.) who was blinded to the genotype of the mice. Comparisons for degree of potentiation were made between the average of 10 responses immediately preceding the tetanic stimulus and the 10 responses between 50 and 60 min after the tetanus. Statistical comparisons between groups were made using Student's t test.

RESULTS

Generation of GFAP-Null Mice. GFAP-null mice were generated by gene targeting in embryonic stem cells. Fig. 1*A* illustrates the wild-type *Gfap* locus (*top*), the targeting vector (*middle*), the mutant *Gfap* locus (*bottom*), and the probes used for genotyping in Southern blots. The majority of exon 1 and all of exons 2–4 were replaced in the targeting vector by the *neo* cassette. Following electroporation of the targeting vector into ES cells, 518 clones were isolated that were doubly resistant to G418 and FIAU. Eight of these clones contained the disrupted *Gfap* locus, based upon Southern blot analysis as described in the *Material and Methods* (data not shown). Three clones (K19, K20, and K21) were used to generate chimeric founder mice, and representatives of all three clones successfully transmitted the mutant allele to heterozygous offspring. Heterozygotes were interbred to produce homozygous mutant mice, and Fig. 1*B* shows a Southern blot analysis of tail biopsies taken from one such litter at weaning. These crosses yielded the expected Mendelian ratios of wild-type, heterozygous, and homozygous mutant mice.

From birth onward, the overt appearance of the homozygous mutant mice was indistinguishable from their heterozygous and wild-type littermates. Mutant mice reached sexual maturity and were fertile. The oldest mice in our colony are now 14 months old, and show no evidence of a shortened lifespan. The same apparent lack of developmental consequences of the GFAP mutation was observed in mice derived from all three independently-derived clones, and in either the 129 or hybrid B6/129 genetic backgrounds. For detailed analysis we concentrated on mice derived from one clone, K19.

Absence of GFAP and Lack of Compensation by Other Intermediate Filaments in Homozygous Mutant Mice. To verify that the homozygous mutant mice produced no GFAP, we assayed for both GFAP mRNA and protein. Northern blot analysis confirmed the absence of GFAP mRNA in the homozygous mutant mice (hereafter referred to as GFAP-null), and a reduced level in the heterozygous mice (Fig. 2, *top*). In addition, immunohistochemical studies showed that the GFAP-null mice contained no detectable GFAP protein (see Fig. 3*D*). Northern blot analysis also showed that no compensatory increase occurred in the expression of mRNA for either vimentin (Fig. 2, *middle*) or nestin (Fig. 2, *bottom*), two other intermediate filaments that are expressed in astrocytes, or their precursors (21–24). Immunohistochemical studies of vimentin in brain and optic nerve also showed no evident compensation at the protein level (data not shown).

Light Microscopic Evaluation of CNS. Examination of the brains and retinae of GFAP-null and control mice at the light microscopic level in H&E-stained paraffin sections revealed

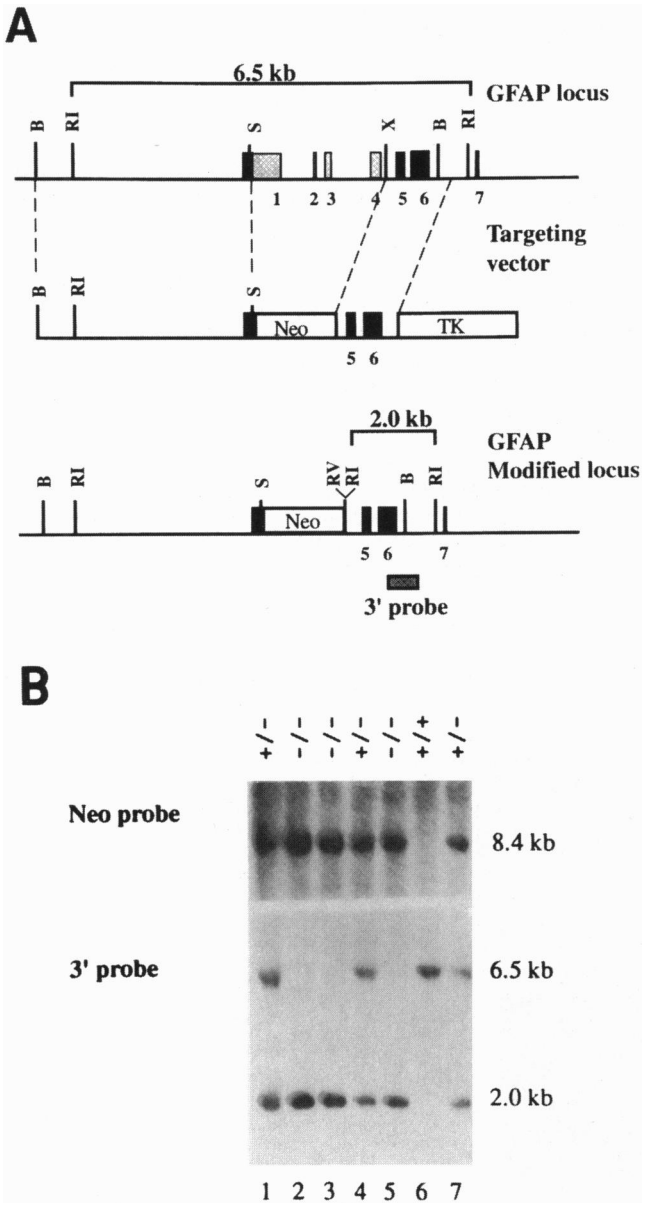

FIG. 1 (*A*) The *Gfap* gene, targeting vector, and modified *Gfap* gene. (*Top*) The wild-type *Gfap* locus is illustrated with the first seven of its nine exons (boxes) labeled below. The exons represented by stippled boxes (most of exon 1, exons 2–4) are replaced in the targeting vector (*middle*) by a PGK-*neo* cassette. The 2.2-kb 5′ arm of homology and the 1.4-kb 3′ arm of homology are shown delimited by dashed lines connecting the wild-type locus with the targeting vector. The diagram at the bottom illustrates the predicted modified locus after homologous recombination and Southern blot strategy for genotyping cells and mice. A probe from the *neo* gene served to verify appropriate recombination within the 5′ arm of homology. A *Bam*HI–*Eco*RI GFAP 3′ fragment (outside the arm of homology in the targeting vector) distinguished the wild-type *Eco*RI band (6.5 kb) from the mutant band (2.0 kb), due to the extra *Eco*RI site introduced as part of the *neo* cassette, and verified appropriate recombination within the 3′ arm of homology. (*B*) In the Southern blot at the top, an 8.4-kb *Eco*RV fragment from mice that have inherited one or two copies of the mutant allele hybridizes to the *neo* probe (+/− and −/−; lanes 1–5 and 7), whereas the wild-type mouse (+/+; lane 6) does not carry the *neo* gene. In the Southern blot (*bottom*), the 3′ GFAP probe hybridizes either to a 6.5-kb *Eco*RI fragment from the wild-type allele, or to a 2.0-kb fragment from the mutant allele. Wild-type mice (lane 6) showed only the 6.5-kb band, heterozygous mice (+/−; lanes 1, 4, and 7) showed both 6.5- and 2-kb bands, and homozygous mutant mice (−/−; lanes 2, 3, and 5) showed only one band at 2.0 kb.

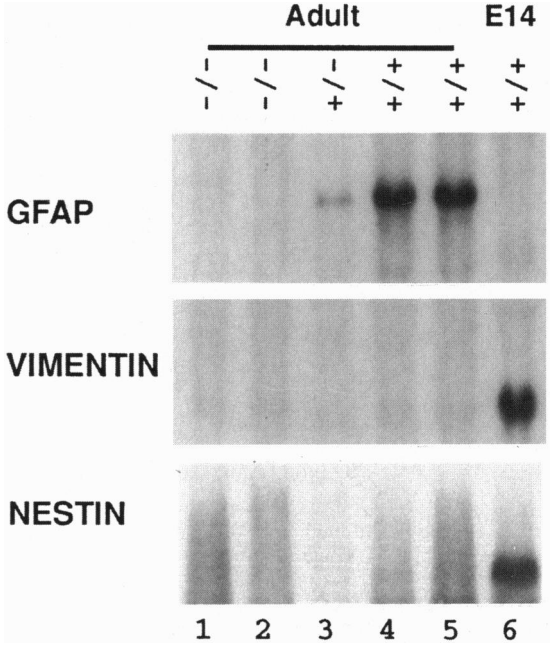

FIG. 2. Northern blot analysis of mRNAs for GFAP, vimentin, and nestin in whole brains of adult wild-type, heterozygous, and GFAP-null mice. For GFAP (*top*), a single band was present in RNA from wild-type (lanes 4 and 5) and heterozygous (lane 3) mice, but was absent from GFAP-null mice (lanes 1 and 2). Because ethidium bromide staining of the gel indicated approximately equal loading of RNA in each lane (data not shown), the heterozygote appears to have reduced levels of GFAP mRNA compared to wild type. No up-regulation of vimentin (*middle*) or nestin (*lower*) is evident in either the heterozygote or GFAP-null mice. Because vimentin and nestin are only expressed at low levels in adult mice, an embryonic day 14 (E14) mouse sample was included as a positive control for these mRNAs. GFAP was not detectable in E14 wild-type mice (lane 6).

no obvious abnormalities resulting from the absence of GFAP expression. Sagittal sections through the hippocampus of a 40-day-old wild-type mouse and a GFAP-null mouse, stained with H&E, are shown in the low power photomicrographs in Fig. 3 *A* and *B*) to illustrate a region of the CNS that normally contains numerous astrocytes. Stratification of neurons into the densely packed stratum pyramidale of the hippocampus and granule cell layer of the dentate gyrus appeared normal. Adjacent sections from the same animals were reacted with a polyclonal antisera to GFAP. Whereas GFAP-immunoreactive astrocytes were normally distributed throughout the hippocampus of wild-type mice (Fig. 3*C*), no immunoreactive cells were seen anywhere in the hippocampus of GFAP-null mice (Fig. 3*D*). Examination of other regions of the CNS of GFAP-null mice also failed to detect any GFAP-immunoreactivity (data not shown). GFAP-null astrocytes also failed to stain with a monoclonal antibody (GA5) specific for the carboxyl-terminal of the protein (25) (data not shown).

Ultrastructural Evaluation of Astrocytes and Nonmyelinating Schwann Cells. To evaluate further the morphology of astrocytes in the GFAP-null mice, we examined transverse sections of optic nerve by electron microscopy (Fig. 4 *A–D*). Astrocytes in wild-type mice are easily identified by their large, elongated profiles and the presence of intermediate filaments. We initially focused on the pial surface (Fig. 4 *A* and *B*), where astrocyte processes containing abundant intermediate filaments normally collect to form the glial limitans. In the GFAP-null mice, putative astrocytes were identified by nuclear morphology, presence of glycogen particles in the cytoplasm, and characteristic sub-plasmalemmal densities. The GFAP-null processes at the pial surface were much smaller than normal, and contained few if any intermediate filaments

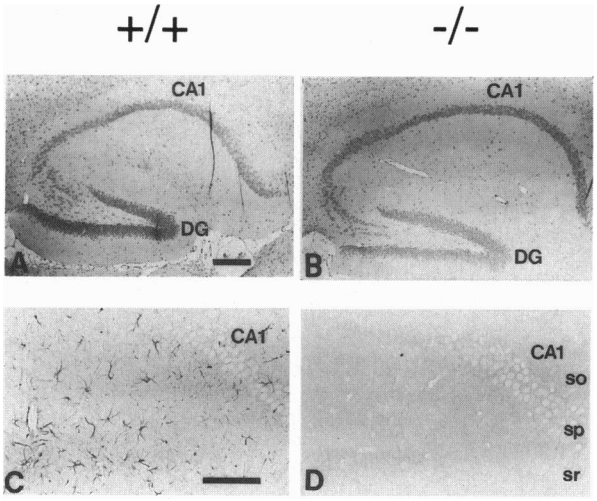

FIG. 3. Histology and immunohistochemistry of hippocampus of wild-type (+/+) and GFAP-null mice (−/−). (*A* and *B*) Low-power photomicrographs of H&E-stained paraffin sections showing normal hippocampal cytoarchitecture. DG, dentate gyrus. (Bar = 250 μm.) (*C* and *D*) Photomicrographs of the CA1 region of hippocampus in GFAP-immunostained paraffin sections. Cell bodies of pyramidal neurons in the stratum pyramidale are in the upper right corner of each field. Note the abundant GFAP-immunoreactive astrocytes in the stratum oriens (so), stratum pyramidale (sp), and stratum radiatum (sr) of the wild-type mouse, but the lack of any GFAP-immunoreactive cells in the GFAP-null mouse. (Bar = 100 μm.)

(Fig. 4*B*). In addition, we examined the astrocyte end-feet on capillary walls, because of the proposed role that astrocytes play in inducing the blood-brain barrier in endothelium (Fig. 4 *C* and *D*). GFAP-null astrocytes do form end-feet, and many of these distal processes contain intermediate filaments (Fig. 4*D*) (note also the occasional intermediate filament-containing processes in Fig. 4*B*). However, in other areas of the optic nerve, it was difficult to find any processes containing intermediate filaments, and presumed astrocyte processes were smaller than in wild-type mice. The CA1 region of the hippocampus was also examined at the ultrastructural level, but intermediate filament-containing astrocyte processes were scarce even in the control mice and there were no obvious differences between mutants and controls (data not shown).

To evaluate the morphology of nonmyelinating Schwann cells, a GFAP-expressing glial cell in the peripheral nervous system, we examined transverse sections of sciatic nerve. Nonmyelinating Schwann cells in wild-type mice contain few intermediate filaments, but form delicate processes separating individual small-diameter axons (Fig. 4*E*). The nonmyelinating Schwann cells of the GFAP-null mice formed the same type of processes, and also segregate axons into individual compartments (Fig. 4*F*).

Synaptic Transmission and LTP in the Hippocampus. Changes in astrocyte morphology near synapses have been observed following learning tasks and after induction of LTP (26, 27). To test whether the absence of GFAP alters the ability of synapses to undergo plastic changes, we measured extracellular responses to Schaffer collateral stimulation in the hippocampal CA1 region before and for 1 hr following an LTP-inducing stimulus in a group of wild-type (n = 6 mice, 10

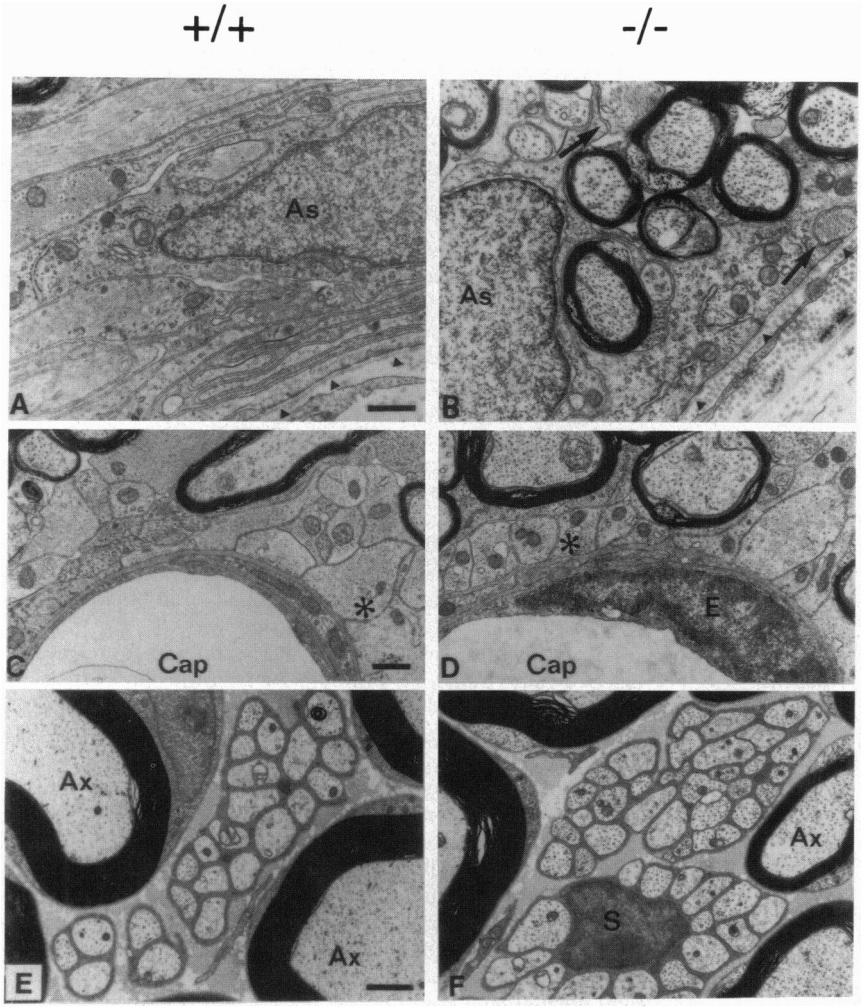

FIG. 4. Ultrastructure of optic nerves of wild-type (+/+) and GFAP-null mice (−/−). (*A* and *B*) Transverse sections of optic nerve showing astrocyte cell bodies with nuclei (As) and astrocyte processes with associated basal lamina of the glial limitans (arrowheads). In the wild-type mouse, note the numerous astrocytic processes filled with intermediate filaments cut in both longitudinal and transverse orientations. In the GFAP-null mouse, astrocytes are present and form a glial limitans (note basal lamina), but contain few if any intermediate filaments. However, some astrocyte processes of the GFAP-null mouse do contain intermediate filaments (arrows). (Bar = 0.5 μm.) (*C* and *D*) Transverse sections of optic nerves showing distal processes of astrocytes forming end-feet (some marked by asterisks) in contact with capillary walls (Cap, capillary lumen; E, nucleus of endothelial cell). Note the presence of some residual intermediate filaments in the end-feet of the GFAP-null mouse. (Bar = 0.5 μm.) (*E* and *F*) Transverse sections of sciatic nerves showing clusters of small-diameter axons and apparently normal ensheathment by nonmyelinating Schwann cells of the GFAP-null mouse. Nucleus of a nonmyelinating Schwann cell (S) is present in *F*. Large-diameter myelinated axons surround these clusters (Ax). (Bar = 1 μm.)

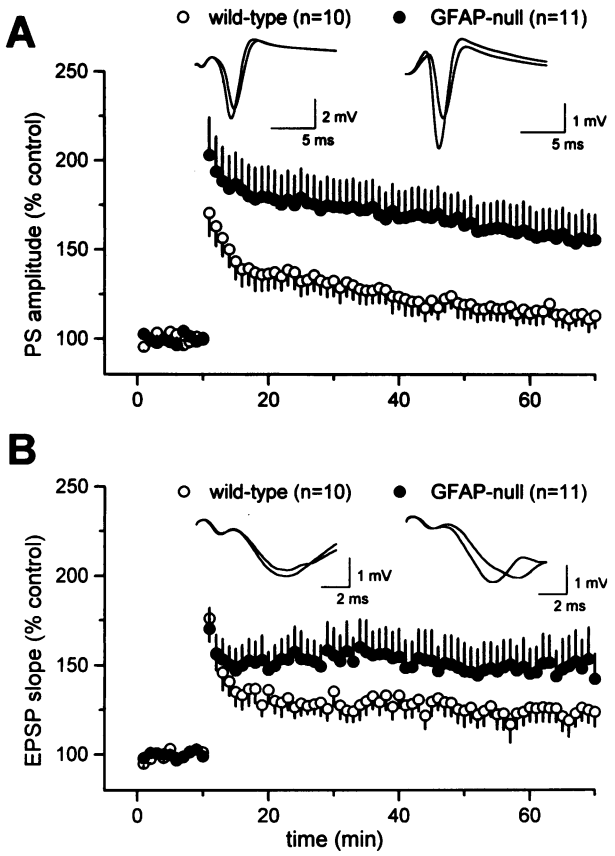

FIG. 5. LTP is enhanced in GFAP-null mice. Population spike amplitude (*A*) and EPSP slope (*B*) are plotted for the 10 min preceding and 60 min after LTP induction. Data from each slice were normalized to the mean of the 10 responses immediately preceding the stimulus train, and are plotted as means ± standard error (control: 10 slices from 6 mice; mutant: 11 slices from 6 mice). Insets illustrate averaged responses to 10 stimuli for typical mutant and wild-type slices, immediately before and 60 min after LTP induction. Calibration bars: *A*, 2 mV, 5 ms (control) and 1 mV, 5 ms. GFAP-null: *B*, 1 mV, 2 ms (both).

slices) and GFAP-null (n = 6 mice, 11 slices) mice. No difference between groups was observed in either PS amplitude (wild type = 2.2 ± 0.8 mV versus GFAP-null = 2.7 ± 0.8 mV, mean ± SD, $P > 0.10$) or EPSP slope (wild type = −1.7 ± 1.6 mV/ms versus GFAP-null = −1.3 ± 1.3 mV/ms, $P > 0.10$) under baseline recording conditions. Following tetanus, LTP of both the PS and EPSP was observed in 6 of 10 slices from wild-type and in 9 of 11 slices from GFAP-null mice. In addition, one wild-type and one GFAP-null slice showed LTP of the PS only, and two wild-type slices showed LTP of the EPSP only. A significantly larger increase in amplitude of the PS was observed in the GFAP-null group than in the wild-type mice (Fig. 5*A*), whether comparing all animals (wild type = 114 ± 21% versus GFAP-null = 156 ± 49%, $P < 0.05$) or only those animals that showed potentiation of both PS and EPSP slope (wild type = 120 ± 10% versus GFAP-null = 167 ± 48%, $P < 0.05$). Differences between groups were apparent immediately following the tetanus, and persisted for the duration of the experiments (1 hr). In addition, EPSP slope was increased to a greater degree in GFAP-null mice than in wild type (Fig. 5*B*), although the difference did not reach statistical significance when results from all animals were compared (wild type = 124 ± 24% versus GFAP-null = 149 ± 52%, $P = 0.09$). When only those animals that showed potentiation of both PS and EPSP slope were considered, EPSP slope was significantly greater 1 hr following tetanus in the GFAP-null group (wild type = 127 ± 23% versus GFAP-null = 161 ± 48%, $P < 0.05$). Thus, GFAP-null mice display enhanced synaptic plasticity compared to wild-type controls, both of the population EPSP and of the PS.

DISCUSSION

We have created mice carrying a null mutation in the *Gfap* gene that are completely deficient in GFAP message and protein. While our work was in progress, papers appeared from two other groups also describing GFAP-null mice (12, 13) [a third has been presented in abstract form (28)]. The results from these other laboratories are similar to ours in observing that GFAP-null mice are indistinguishable from their wild-type littermates in their development, fertility, and gross CNS morphology and behavior. Our data show that this absence of an obvious phenotype is not due to compensatory up-regulation of vimentin or nestin. Similarly, Gomi *et al.* (12) found no compensation by vimentin as measured at the protein level in SDS/PAGE, and Edelmann *et al.* (28) failed to find compensation using a pan-intermediate filament antibody. While no GFAP can be detected and no vimentin or nestin up-regulation occurs, some intermediate filaments can still be seen in the optic nerve astrocytes of our GFAP-null mice, particularly in the distal portions of the processes forming end-feet on capillaries. In contrast, Pekny *et al.* (13) report that intermediate filaments are completely absent in their GFAP-null mice, both in the lateral funiculus of the spinal cord and the dentate gyrus of the hippocampus. The reason for the difference between these results is not known, but could reflect anatomic variation in the sites being examined. The mice described by Edelmann *et al.* (28) also contain residual intermediate filaments in optic nerve astrocytes, but lack them in spinal cord (Liedtke, W. and Raine, C. S., personal communication). The identity of the residual filaments we observed remains to be determined, but a likely candidate is vimentin, an intermediate filament normally expressed in astrocytes or their precursors. It is of interest that vimentin-deficient mice also are viable and fail to show evidence of compensation by other intermediate filaments (29). Evidently, many cell types can maintain gross function without their normal complement of intermediate filaments. It will be of interest to determine the effects of producing mice carrying mutations in multiple intermediate filament genes.

In none of the studies of GFAP-null mice has the morphology of the astrocytes been evaluated in detail, a task made difficult by the absence of GFAP as a cell marker. We have shown that astrocytes in the optic nerve extend processes appropriate distances to the glial limitans and capillary walls, but that their caliber appears diminished. In this respect, the phenotype of this intermediate filament mutation may resemble that seen in disorders of neurofilaments, where axons reach their targets despite having smaller cross-sectional diameters (30, 31). This alteration in astrocyte processes does not appear to affect the blood-brain barrier, an endothelial function thought to be induced by contact with astrocytes (32), as Pekny *et al.* (13) found no leakage of Evans Blue following its intravenous administration. This absence of an effect on the blood-brain barrier is consistent with recent studies of astrocyte development by Zerlin *et al.* (33), who showed that contact of capillary walls by astrocytes occurs early in differentiation, prior to expression of GFAP.

Another CNS function that could be affected by a change in astrocyte processes is synaptic transmission. Astrocyte processes are intimately associated with the synaptic cleft, where they may regulate synaptic function through uptake of neurotransmitters, buffering of cations and pH, and presenting barriers for diffusion of calcium. For example, Smith (34) calculated that a widening of the distance between the astrocytic processes and the synapse by approximately 10 nm (which would have been undetected in our studies) could increase

presynaptic transmitter release by ≈200%. In addition, morphometric studies have shown dynamic changes in glial morphology following induction of LTP or in association with a learning task (26, 27).

LTP is defined as a long-lasting enhancement of synaptic efficacy following tetanic stimulation. However, there is considerable controversy over the site of this enhancement (35). Most of the theoretical and experimental studies of LTP have focused on the isolated role of neurons, with relatively little attention to the associated glia. In fact, all of the recent gene knockouts that have investigated LTP have involved neuronally expressed genes and resulted in impaired LTP (36–42). When we analyzed synaptic function in our GFAP-null mice, we found that baseline synaptic transmission was unaffected in the mutant mice, but that LTP was enhanced. The degree of potentiation in the wild-type mice was small, presumably due to the use of a relatively weak (submaximal) potentiating stimulus intensity. Also, no GABAA receptor antagonists such as picrotoxin, which are often used to enhance the expression of LTP, were included in these experiments. However, these factors are unlikely to have produced the difference in LTP that was observed, because the same stimulus paradigm was used for both groups of mice.

Our results thus imply a role for astrocytes in LTP. One possibility is that their role is indirect; for example, through a developmental effect on neurons. Astrocytes are a source of numerous neurotrophic factors (43, 44), and an absence of GFAP might interfere with their production. Another possibility is that GFAP directly participates in the changes in glial processes that have been associated with LTP (26). Of possible relevance, Steward *et al.* (45) have shown that GFAP expression itself is regulated by neuronal activity, and it is possible that astrocytes undergo rapid changes in shape similar to those observed in neuronal dendritic spines (46). Such rapid changes have been documented in astrocytes of the chicken cochlear nucleus (47). It will be interesting to see whether GFAP-null mice demonstrate physiological changes in other areas of the CNS and in other neuronal phenomena, such as LTD. The link established here between LTP and GFAP promises to provide a new avenue for discoveries concerning astrocyte-neuronal interactions.

We thank Allan Bradley for the AB-1 cells; Paul Hasty, Virginia Lee, and Ron McKay for plasmids; Lew Haberly and Alan Fine for comments on the LTP data; and Heide Peickert, Denice Springman, Carol Gabel, and Dace Klimanis for technical assistance. This work was supported by research grants from the National Institutes of Health (A.M., S.Y.C., R.R.B., and R.A.P.) and the National Multiple Sclerosis Society (A.M.). A.M. is a Shaw Scholar of the Milwaukee Foundation.

1. Murphy, S., ed. (1993) *Astrocytes: Pharmacology and Function* (Academic, San Diego), pp. 1–457.
2. Dahl, D. (1981) *J. Neurosci. Res.* **6,** 741–748.
3. Bovolenta, P., Liem, R. K. H. & Mason, C. A. (1984) *Dev. Biol.* **102,** 248–259.
4. Cochard, P. & Paulin, D. (1984) *J. Neurosci.* **4,** 2080–2094.
5. Barber, P. C. & Lindsay, R. M. (1982) *Neuroscience* **7,** 3077–3090.
6. Jessen, K. R. & Mirsky, R. (1984) *J. Neurocytol.* **13,** 923–934.
7. Feinstein, D. L., Weinmaster, G. A. & Milner, R. J. (1992) *J. Neurosci. Res.* **32,** 1–14.
8. Eng, L. F. & Ghirnikar, R. S. (1994) *Brain Pathol.* **4,** 229–237.
9. Weinstein, D. E., Shelanski, M. L. & Liem, R. K. H. (1991) *J. Cell Biol.* **112,** 1205–1213.
10. Rutka, J. T. & Smith, S. L. (1993) *Cancer Res.* **53,** 3624–3631.
11. Chen, W.-J. & Liem, R. K. H. (1994) *J. Cell Biol.* **127,** 813–823.
12. Gomi, H., Yokoyama, T., Fujimoto, K., Ideka, T., Katoh, A., Itoh, T. & Itohara, S. (1995) *Neuron* **14,** 29–41.
13. Pekny, M., Levéen, P., Pekna, M., Eliasson, C., Berthold, C.-H., Westermark, B. & Betsholtz, C. (1995) *EMBO J.* **14,** 1590–1598.
14. Soriano, P., Montgomery, C., Geske, R. & Bradley, A. (1991) *Cell* **64,** 693–702.
15. Ramírez-Solis, R., Davis, A. C. & Bradley, A. (1993) *Methods Enzymol.* **225,** 855–878.
16. Ausubel, F. M., Brent, R., Kingston, R. E., Moore, D. D., Seidman, J. G., Smith, J. A. & Struhl K. (1988) *Current Protocols in Molecular Biology* (Wiley, New York).
17. Lewis, S. A., Balcarek, J. M., Krek, V., Shelanski, M. & Cowan, N. J. (1984) *Proc. Natl. Acad. Sci. USA* **81,** 2743–2746.
18. Hirschhorn, R. R., Aller, P., Yuan, Z. A., Gibson, C. W. & Baserga, R. (1984) *Proc. Natl. Acad. Sci. USA* **81,** 6004–6008.
19. Lendahl, U., Zimmerman, L. B. & McKay, R. D. G. (1990) *Cell* **60,** 585–595.
20. Pleasure, S. J., Lee, V. M.-Y. & Nelson, D. L. (1990) *J. Neurosci.* **10,** 2428–2437.
21. Dahl, D., Bignami, A., Weber, K. & Osborn, M. (1981) *Exp. Neurol.* **73,** 496–506.
22. Fedoroff, S., White, R., Neal, J., Subrahmanyan, L. & Kalnins, V. I. (1983) *Dev. Brain Res.* **7,** 303–315.
23. Pixley, S. K. R. & de Vellis, J. (1984) *Dev. Brain Res.* **15,** 201–209.
24. Clarke, S. R., Shetty, A. K., Bradley, J. L. & Turner, D. A. (1994) *NeuroReport* **5,** 1885–1888.
25. Debus, E., Weber, K. & Osborn, M. (1983) *Differentiation* **25,** 193–203.
26. Wenzel, J., Lammert, G., Meyer, U. & Krug, M. (1991) *Brain Res.* **560,** 122–131.
27. Anderson, B. J., Li, X., Alcantara, A. A., Isaacs, K. R., Black, J. E. & Greenough, W. T. (1994) *Glia* **11,** 73–80.
28. Edelmann, W., Roback, L., Chiu, F.-C., Kress, Y., Wainer, B. & Kucherlapati, R. (1995) *J. Neurochem.* **64,** Suppl., S85 (abstr.).
29. Colucci-Guyon, E., Portier, M.-M., Dunia, I., Paulin, D., Pournin, S. & Babinet, C. (1994) *Cell* **79,** 679–694.
30. Ohara, O., Gahara, Y., Miyake, T., Teraoka, H. & Kitamura, T. (1993) *J. Cell Biol.* **121,** 387–395.
31. Eyer, J. & Peterson, A. (1994) *Neuron* **12,** 389–405.
32. Janzer, R. C. & Raff, M. C. (1987) *Nature (London)* **325,** 253–257.
33. Zerlin, M., Levison, S. W. & Goldman, J. E. (1995) *J. Neurosci.* **15,** 7238–7249.
34. Smith, S. J. (1992) *Prog. Brain Res.* **94,** 119–136.
35. Bliss, T. V. P. & Collingridge, G. L. (1993) *Nature (London)* **361,** 31–39.
36. Grant, S. G. N., O'Dell, T. J., Karl, K. A., Stein, P. L., Soriano, P. & Kandel, E. R. (1992) *Science* **258,** 1903–1910.
37. Silva, A. J., Stevens, C. F., Tonegawa, S. & Wang, Y. (1992) *Science* **247,** 201–206.
38. Abeliovich, A., Chen, C., Goda, Y., Silva, A. J., Stevens, C. F. & Tonegawa, S. (1993) *Cell* **75,** 1253–1262.
39. Collinge, J., Whittington, M. A., Sidle, K. C. L., Smith, C. J., Palmer, M. S., Clarke, A. R. & Jefferys, J. G. R. (1994) *Nature (London)* **370,** 295–297.
40. Conquet, F., Bashir, Z. I., Davies, C. H., Daniel, H., Ferraguti, F., Bordi, F., Franz-Bacon, K., Reggiani, A., Matarese, V., Condé, F., Collingridge, G. L. & Crépel, F. (1994) *Nature (London)* **372,** 237–243.
41. Korte, M., Carroll, P., Wolf, E., Brem, G., Thoenen, H. & Bonhoeffer, T. (1995) *Proc. Natl. Acad. Sci. USA* **92,** 8856–8860.
42. Sakimura, K., Kutsuwada, T., Ito, I., Manabe, T., Takayama, C., Kushiya, E., Yagi, T., Aizawa, S., Inoue, Y., Sugiyama, H. & Mishina, M. (1995) *Nature (London)* **373,** 151–155.
43. Rudge, J. S., Alderson, R. F., Pasnikowski, E., McClain, J., Ip, N. Y. & Lindsay, R. M. (1992) *Eur. J. Neurosci.* **4,** 459–471.
44. Müller, H. W., Junghans, U. & Kappler, J. (1995) *Pharmacol. Ther.* **65,** 1–18.
45. Steward, O., Torre, E. R., Tomasulo, R. & Lothman, E. (1991) *Proc. Natl. Acad. Sci. USA* **88,** 6819–6823.
46. Hosokawa, T., Rusakov, D. A., Bliss, T. V. P. & Fine, A. (1995) *J. Neurosci.* **15,** 5560–5573.
47. Canady, K. S. & Rubel, E. W. (1992) *J. Neurosci.* **12,** 1001–1009.